DIVALENT CATION AFFINITY SITES

IN *PARAMECIUM AURELIA*

G. FISHER, E. S. KANESHIRO, and P. D. PETERS

From the Department of Biological Sciences, University of Cincinnati, Cincinnati, Ohio 45221 and
The Cavendish Laboratory, Cambridge CB2-3RQ, England. Dr. Peters's present address is
The Botany School, The University of Cambridge, England.

ABSTRACT

Sites with high calcium affinity in *Paramecium aurelia* were identified by high calcium (5 mM) fixation and electron microscope methods. Electron-opaque deposits were observed on the cytoplasmic side of surface membranes, particularly at the basal regions of cilia and trichocyst-pellicle fusion sites. Deposits were also observed on some smooth cytomembranes, within the axoneme of cilia, and on basal bodies. The divalent cations, Mg^{2+}, Mn^{2+}, Sr^{2+}, Ni^{2+}, Ba^{2+}, and Zn^{2+}, could be substituted for Ca^{2+} in the procedure. Deposits were larger with 5 mM Sr^{2+}, Ba^{2+}, and Mn^{2+} at ciliary transverse plates and the terminal plate of basal bodies. Microprobe analysis showed that Ca and Cl were concentrated within deposits. In some analyses, S and P were detected in deposits. Also, microprobe analysis of 5 mM Mn^{2+}-fixed *P. aurelia* showed that those deposits were enriched in Mn and Cl and sometimes enriched in P.

Deposits were seen only when the ciliates were actively swimming at the time of fixation. Locomotory mutants having defective membrane Ca-gating mechanisms and ciliates fixed while exhibiting ciliary reversal showed no obvious differences in deposition pattern and intensity. Possible correlations between electron-opaque deposits and the locations of intramembranous particles seen by freeze-fracture studies, as well as sites where fibrillar material associate with membranes are considered. The possibility that the action sites of calcium and other divalent cations were identified is discussed.

The role of divalent cations as regulatory agents modifying the ciliary activity of *Paramecium* and other cell types is not clearly understood. However, it has been well established that divalent cations, principally Ca^{2+}, directly or indirectly cause several changes to occur. Studies on the influence of Ca^{2+} on ciliary function have resulted in the following observations: (a) Depolarization of the cell membrane of ciliates which may occur spontaneously or be induced by electrical, chemical, or mechanical stimuli results in increased membrane conductance to Ca^{2+}, Ba^{2+}, or Sr^{2+} (28). External Ca^{2+} concentrations also influence the ionic permeability of the membrane. (b) The increased Ca^{2+} influx along the cation's electrochemical gradient resulting from the membrane conductance changes alters the intracellular (intraciliary) Ca^{2+} concentration which then modifies the orientation of the effective stroke of *Paramecium* ciliary beat (9, 22, 23, 29, 30). (c) Ciliary beat frequency is also regulated by Ca^{2+} (10, 30). (d) The duration of ciliary reversal is

correlated with Ca^{2+} levels (27). (e) Cilia detach from ciliates when cells pretreated with alcohol and chelator are exposed to high concentrations of Ca^{2+} (16, 49).

It is probable that several of these observations reflect the same mechanisms involved in the alteration of ciliary activity. Recently, the use of high Ca^{2+} fixation and electron microscopy has localized electron-opaque deposits in a variety of cell types at sites allegedly involving Ca^{2+} interactions (6, 19, 24, 32, 33, 37, 39, 44). Plattner (37) tested these techniques on P. aurelia. He observed electron-dense deposits and also correlated their presence with membrane-intercalated particles which were arranged in plaques at basal regions of cilia.

The present studies not only confirm many of Plattner's findings but are extended to include additional observations. Various ions were found to substitute for Ca^{2+}. Also, x-ray microprobe analyses confirmed the presence of the cation which was added to fixatives as being concentrated within the electron-opaque deposits. Cells exhibiting different orientations in ciliary beat as well as membrane mutants were compared for deposition differences. A preliminary report on divalent cation affinity sites in P. aurelia has been presented elsewhere (12).

The terminology used in this paper for ciliate structures will conform to that described by Allen (1, 3, 4), Hufnagel (20), and Pitelka (36). The reader is referred to available schematic diagrams of the orientation of Paramecium cortical structures (3, 20).

MATERIALS AND METHODS

Experimental Organisms

Paramecium aurelia strains 299s of syngen 8 and 51s of syngen 4 as well as the pawn mutants, $d_4 94$ and $d_4 95$, derived from 51s (obtained from Dr. C. Kung, University of Wisconsin, Madison, Wisc., and Dr. J. Preer, Indiana University, Bloomington, Indiana) were used in these studies. Pawn mutants, unlike parental type cells, do not exhibit a voltage-dependent increase in calcium conductance and ciliary reversal. Cells were cultured in the dark at 28.5°C or 25°C in either a bacterized cerophyl medium (46) or an axenic crude medium (45) with or without folic acid supplementation (2.5 or 25 µg/ml final concentration). Cultures were maintained in 5 or 10 ml of medium in upright screw-cap culture tubes. Bacterized mass cultures were grown in 1 liter volumes in Fernbach flasks, and axenic mass cultures were grown in 100 ml volumes in 250-ml Erlenmeyer flasks. Late log to early stationary phase cultures were concentrated in a continuous flow cell harvester (7), washed with 2 vol of double-distilled water, and resuspended in 0.07 M morpholinopropane sulfonic acid (MOPS) buffer (pH 7.2-7.4). MOPS buffer was prepared from morpholine and 1,3-propane sulfone (Aldrich Chemical Co., Milwaukee, Wisc.).

Electron Microscope Cytochemistry

Electron-opaque deposits appeared in P. aurelia cells if the ciliates were active when fixed. Moribund and immobile cells did not show deposits. Therefore, cell suspensions were checked for swimming activity before fixation and often allowed to recover from centrifugation. In some experiments the fixative was added directly to cell cultures to avoid centrifugation. The results were similar to those for washed, centrifuged, active cells.

Concentrated cells were fixed at room temperature or at 4°C in glutaraldehyde solutions according to the procedure of Oschman and Wall (33, 34). Sodium ion, K^+, Mg^{2+}, Ca^{2+}, Mn^{2+}, Sr^{2+}, Ba^{2+}, Zn^{2+}, Ni^{2+} (as chloride salts) and $Ca(NO_3)_2$ were added singularly to fixatives to give a final fixation concentration of 5 mM. Fixatives without addition of salts and fixatives with 5 mM disodium ethylenediaminetetraacetic acid (EDTA) were also tested.

Atomic absorption flame photometry (Unicam SP 90, Philips Electronic Instruments, Inc., Mount Vernon, N.Y., operated at 423 nm absorbance maximum) was used to check the final concentrations of Ca^{2+} after the cells were mixed with the fixative. After treatment with 5 mM Ca^{2+}-fixative solutions, the supernate contained 4.6 mM Ca^{2+} (± 0.1 SD, N = 5). After 5 mM Mn^{2+} fixation (here a two times concentrated fixative was mixed 1:1 with the culture medium), the supernate contained < 0.06 mM Ca^{2+} (± 0.03 SD, N = 5).

Fixation times tested ranged from 2 to 24 h. No significant differences were obvious. Use of cacodylate or collidine buffer in the fixation procedure gave similar Ca deposits. Treatment with 5 mM Ca^{2+} was tested for its effects during and after aldehyde fixation. Deposits did not form if Ca^{2+} was introduced after fixing with glutaraldehyde overnight. Other Ca^{2+} concentrations in the fixative, 0.05, 0.5, 50, and 500 mM, were tested. The concentration range from 0.5 to 50 mM gave similar results, which could indicate that sites involved in the formation of deposits were saturated at 0.5 mM Ca^{2+} (37). Fixative solutions containing more than 50 mM Ca^{2+} resulted in broken cells and abnormal morphology. The effects of pH differences were tested from pH 5.5 to 8.5, and no obvious differences were detected. No differences were seen between $Ca(NO_3)_2$ and $CaCl_2$ fixation.

After glutaraldehyde-cation fixation, cells were concentrated into a packed pellet and washed twice in 0.08 M S-collidine buffer washes (pH 7.2-7.4) for 15 min

each. In some cases, 5 mM Ca^{2+} was added to buffer washes but it had no influence on the final deposits observed. The effects of postfixing with osmium tetroxide was tested in some studies, in which cells were treated with 1% OsO_4 for 45 min followed by two more 15-min buffer washes. Osmication, with or without Ca^{2+}, did not dramatically alter the distribution of deposits. Cells were then dehydrated in a series of solutions of increasing ethanol concentrations. Ethanol was replaced by propylene oxide, then the cells were infiltrated in a series of increasing plastic to propylene oxide solutions. Both Epon (25) and Spurr (47) plastics were used, and infiltration times of 12 h to 4 days were tested. Paramecia were found to require the longer infiltration periods of several days. After sufficient infiltration the cells were embedded and the plastic was cured in an oven at 60°C for a minimum of 12 h. Ultrathin and thick sections were cut on an LKB ultramicrotome III (LKB Instruments, Inc., Rockville, Md.) with a diamond knife (DuPont Instruments, Wilmington, Del.) or glass knives and placed on either carbon-coated or uncoated copper grids. Sections were stained with 5% aqueous uranyl acetate for 30-45 min or viewed without staining. In some cases thin sections were counterstained with lead citrate (41). Sections were viewed and micrographs taken on an AEI EM6B electron microscope operated at 60 kV.

Fixation of Backward and Forward Swimming Cells

Single cells of strain 299s were observed under a dissecting microscope and isolated in 0.1-ml fluid in microculture slides for fixation during backward swimming. To induce continuous ciliary reversal (CCR) (17) the ciliate was placed in a stimulation solution of 20 mM NaCl, 0.3 mM $CaCl_2$, and 1 mM MOPS buffer at pH 7.2-7.4 till periodic ciliary reversal (PCR) (17) locomotory behavior disappeared and normal left front spiral swimming (LFS) (17) was established. Then a small amount of high Ca^{2+} fixative (<0.02 ml) was carefully introduced from a syringe at the edge of the well opposite the ciliate. When the cell, displaying LFS swimming, encountered the fixative region (anterior end first), it immediately displayed CCR. Fixative was rapidly added to the well while the cell was displaying this behavior. The same procedure was used on fixation of strain $d_4$95 pawn cells. In this case, however, these ciliates did not exhibit CCR.

Elemental Analysis by X-ray Microprobe

Thick sections (green or blue interference colors) of unstained high Ca^{2+}- and high Mn^{2+}-fixed cells were placed on Formvar plus carbon-coated nickel or copper grids. Specimens were analyzed with an AEI EMMA-4 microprobe analyzer equipped with a Kevex energy dispersive X-ray spectrometer with a Si- (Li) detector (Kevex Corp., Burlingame, Calif.). Column voltage was

set at 40 kV and a current of about 10 nA was used. The spectrometer was set for 30-s counts, 20 eV/channel. A titanium specimen holder was used. The presence of different elements was determined by comparison of emission spectra obtained from probe areas of approx. 2,000 Å diameter over electron-dense deposits and adjacent cellular areas.

RESULTS

Localization of Deposits

Electron-opaque deposits occurred consistently and reproducibly at several sites in 5 mM Ca^{2+}-fixed *P. aurelia*. The deposits occurred on the cytoplasmic side of surface membranes, the terminal plate of the basal bodies of cilia, the transverse plate of the cilium, occasionally within the axoneme of cilia, on trichocyst-surface membrane junctions, and on internal smooth membranes. Deposits within the axoneme had no apparent correlation with dynein arms since only occasional large deposits were found situated over microtubules as well as areas between them. No morphological specificity was apparent with axonemal deposition (Figs. 1 and 2). Cytomembranes which exhibited deposits were found in the region of the cell gullet and near the cell cortex (Figs. 3, 4, and 5). These are sites in ciliates where endocytotic processes involving food vacuole formation and pinocytosis at parasomal sacs are thought to occur (4, 31). Such smooth cytomembranes, therefore, may have physico-chemical characteristics common with surface membranes, on which deposits were more frequently observed.

Deposits on membranes often occurred at bulges. On surface membranes, deposit location and spacing could reflect specific morphological structures such as membrane-membrane links and intramembranous particles (38). Deposits on the surface membrane opposite alveolar septa were commonly seen (Fig. 6). Deposits occurred at trichocyst tip regions where trichocyst, surface, and alveolar membranes are known to be connected (38) (Figs. 7 and 8). Deposits were often found where the surface membrane invaginates and differentiates into parasomal sacs (Figs. 9, 15, and 23). The surface membrane covering the shaft of the cilium (the proximal region of the cilia will be discussed separately below) as well as other membrane profiles often had deposits at approx. 150 nm spacings. The deposits may represent specific regular membrane substructures (Fig. 10 and Fig. 11 (arrows)).
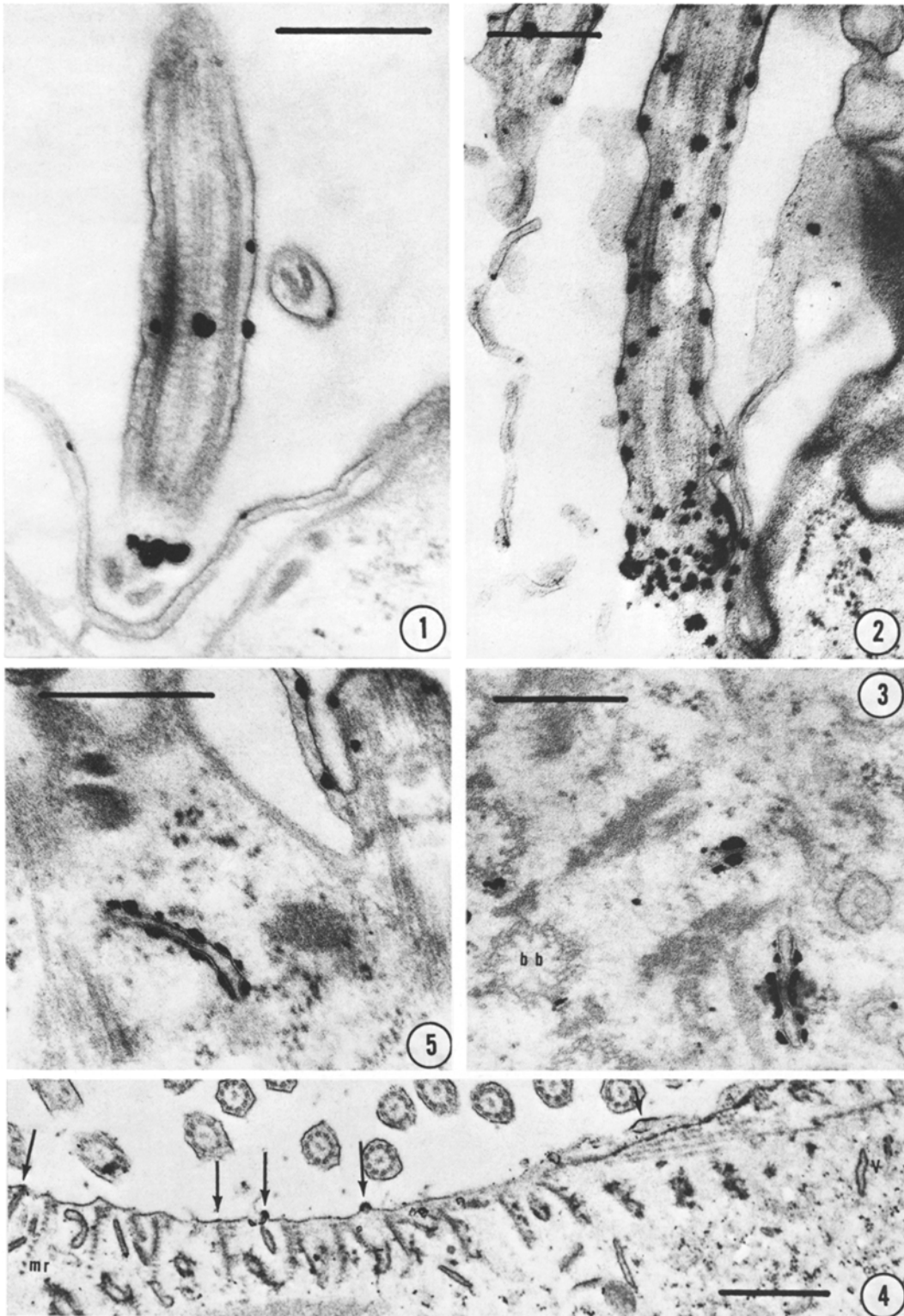
The transition zone of the cilium (Figs. 1, 2, and 11) and the terminal plate of the basal body, which is contiguous with the epiplasm (3, 20), showed large deposits (Figs. 12 and 14–18). Also, the transverse plate, at the level where the two central microtubules of the axoneme appear, had deposits (arrow, Fig. 12). Deposits were often seen opposite microtubular outer doublets. In favorable cross sections nine deposit aggregates were readily distinguished, many in register with the outer doublet microtubules (Fig. 13). Some of these aggregates appeared to be composed of several smaller deposits (arrows, Fig. 13) and may be correlated with individual intramembranous particles of plaques or fibrillar structures present at these loci (37).

The terminal plate of the basal body showed large deposits particularly when fixed in 5 mM Mn^{2+}, Ba^{2+}, or Sr^{2+} (ion substitution studies are described below) (Figs. 14–18). Deposits had a ninefold pattern at the periphery, filling areas between the alveolar membranes and microtubular sets (arrow, Fig. 15). Since the subfibers of the microtubular triplets of the basal body end at the terminal plate, deposits were observed to span areas from membranes to doublets or triplets, depending on whether the plane of the cross section was above or below the terminal plate (see longitudinal section in Figs. 12, 16, and 18).

Deposits were in register with "fuzzy linkers" (43) which have been observed in terminal plates of Tetrahymena cilia and which may also be present in Paramecium. However, in some cross sections, within the transition zone, deposits were also seen between linkers (Fig. 19). Thus, deposits of divalent cations were observed on linker sites in some micrographs (Fig. 13) and in the areas between the linkers in other micrographs (Fig. 19). Within the lumen of the terminal plate, just within the circle of microtubules, a ring of large deposits appeared (Figs. 15 and 17). These may represent deposits on fibrils connecting microtubular sets (43), the arms of the lacy nine-pointed star of the terminal plate lumen (2, 43) or the areas between the arms.

Ion Substitution Studies

Ciliates treated with fixative without ion supplementation or containing the chelator, EDTA, did not contain electron-opaque deposits. Also, cells fixed overnight with 5 mM Na^+ or K^+ did not contain deposits. Magnesium caused fewer deposits, and these were sometimes larger than Ca deposits (Fig. 20). Nickel and Zn deposits had characteristics and distributions similar to those of deposits formed with Ca^{2+} (Figs. 21 and 22).

FIGURE 1   Longitudinal section of cilium of P. aurelia 299s fixed with 5 mM Ca^{2+}. Large electron-opaque deposits coalesce at basal region, and others are seen along ciliary shaft associated with the axoneme as well as surface membrane. Section stained with uranyl acetate. × 47,600. Bar represents 0.5 μm.

FIGURE 2   Longitudinal section of cilium of P. aurelia 299s. Cell fixed at pH 8.5 in 5 mM Ca^{2+}-glutaraldehyde fixative. Deposits are concentrated at base of cilium, and deposits seen on the shaft occur on cytoplasmic face of surface membrane and at random over the axonemal components. Deposits did not differ when cells were fixed at pH 5.5–8.5. Section stained with uranyl acetate and lead citrate. × 34,000. Bar represents 0.5 μm.

FIGURE 3   Section through oral region of P. aurelia 299s fixed with 5 mM Ca^{2+}. Membrane-bounded vesicles or elements of smooth reticulum in this area have deposits. Deposits are seen on outside face of vesicles as would be expected if surface membranes with deposits on cytoplasmic faces were internalized. Cross section of basal bodies (bb) of cilia within complex oral membranelle. Section stained with uranyl acetate. × 36,800. Bar represents 0.5 μm.

FIGURE 4   Section through oral region of P. aurelia 299s fixed with 5 mM Mn^{2+}. Disc-shaped vesicles (v) have deposits on their membranes. Certain regions on cytopharyngeal membrane are also coated with deposits (arrows). Microtubular ribbons (mr) can be seen in this section oriented normal to cytopharyngeal membrane. Section stained with uranyl acetate. × 34,500. Bar represents 1.0 μm.

FIGURE 5   Section of region immediately under cortex of P. aurelia 299s fixed in 5 mM Ca^{2+}. Smooth pair of cytomembranes show deposits. Such smooth membranes could represent vesicles internalized by pinocytotic process at parasomal sacs adjacent to ciliary bases. Section stained with uranyl acetate. × 48,300. Bar represents 0.5 μm.

Strontium, Ba, and Mn deposits were also similar to those formed by Ca^{2+} but were more intense at the terminal plate. Also, in the transition zone of the cilium, distal to the terminal plate, Sr, Ba, and Mn deposits most often appeared as numerous, small, individual units when compared to the larger deposits seen with Ca^{2+} (cf. deposits on the cilium on the left in Fig. 23 with those in Figs. 13 and 19).

Normal cells which were fixed while swimming backward showed no obvious differences in Ca deposits. Pawn cells, which are membrane mutants, contained deposits on surface membranes (Fig. 24).

Microprobe Analysis

Emission spectra indicated that the deposits were enriched in Ca and Cl when compared to background levels from cellular areas without deposits (Figs. 25 and 26). Sulfur and P were concentrated in deposits in some analyses (Figs. 25-30). In materials which were prepared by 5 mM Mn^{2+} fixation, the deposits were enriched in Mn and Cl. Sometimes, deposits showed P enrichment. In deposits caused by 5 mM Mn^{2+} fixation, Ca was not detected (Figs. 29 and 30). This material

(Figs. 29 and 30) was prepared from unwashed cells exposed to 5 mM Mn^{2+} (the fixative solution contained less than 0.06 mM Ca^{2+}). The absence of Ca^{2+} in these deposits indicated that deposits form from the cation that was present in millimolar amounts in the fixative. The K_α and K_β emissions from the specimen holder are seen in each spectrum. Silicon was detected, whether or not deposits were included in the probed area, and is probably a contaminant, possibly from the vacuum pump oil of the instrument.

DISCUSSION

The Ca^{2+}-glutaraldehyde fixation technique for electron microscope cytochemistry (33) has revealed dense deposits associated with a variety of membranes and other cellular sites. The deposits have been found in areas in which physiological studies have implicated Ca^{2+} in the control of cellular processes such as excitation-secretion coupling at the synapse (6, 19, 39), excitation-contraction coupling at the transverse tubules of striated muscles (39), the platelet release reaction (44), control of cell-cell coupling (24), and ciliary activity modification (12, 37). While the physiological significance of the deposits is unclear at present, it is becoming apparent that they represent some

FIGURE 6   A deposit occurs on surface membrane opposite alveolar septum of *P. aurelia* 299s fixed in 5 mM Ca^{2+}. × 35,900. Bar represents 0.5 μm.

FIGURE 7   Unstained section of *P. aurelia* d₄95 fixed in 5 mM Ba^{2+}. Cross-sectional profiles of trichocyst tips show deposits where surface membrane-alveolar membrane connections occur (outer ring) and trichocyst membrane-surface membrane connections occur (inner ring). × 25,700. Bar represents 0.5 μm.

FIGURE 8   Section through a trichocyst tip of *P. aurelia* 51s fixed in 5 mM Ca^{2+}. Deposits are seen where surface membrane-alveolar membrane connections occur. Section stained with uranyl acetate. × 63,000. Bar represents 0.25 μm.

FIGURE 9   Section showing parasomal sac (*ps*) of *P. aurelia* 299s fixed in 5 mM Ca^{2+}. Deposits occur on this membrane which is an invagination of surface membrane at base of cilium. Also see Figs. 15 and 23 for parasomal sac deposits. Section stained with uranyl acetate. × 60,400. Bar represents 0.25 μm.

FIGURE 10   Deposits on surface membranes were often seen with a periodicity of approx. 150 nm. These may be correlated with specific membrane substructures that occur at regular intervals. Micrograph taken of a section of pellicle of *P. aurelia* 299s fixed in 5 mM Ca^{2+}. Section stained with uranyl acetate. × 26,100. Bar represents 0.5 μm.

FIGURE 11   Longitudinal section of cilium of *P. aurelia* 299s fixed in 5 mM Ca^{2+}. Deposits (arrows) can be seen spaced apart at regular intervals. × 28,100. Bar represents 0.5 μm.

FIGURE 12   Longitudinal section of basal region of cilium of *P. aurelia* 299s fixed in 5 mM Ba^{2+}. Terminal plate of basal body has many deposits, and transverse plate of cilium (arrows) where the two central microtubules of the axoneme appear also has deposits. Section stained with uranyl acetate and lead citrate. × 48,000. Bar represents 0.25 μm.
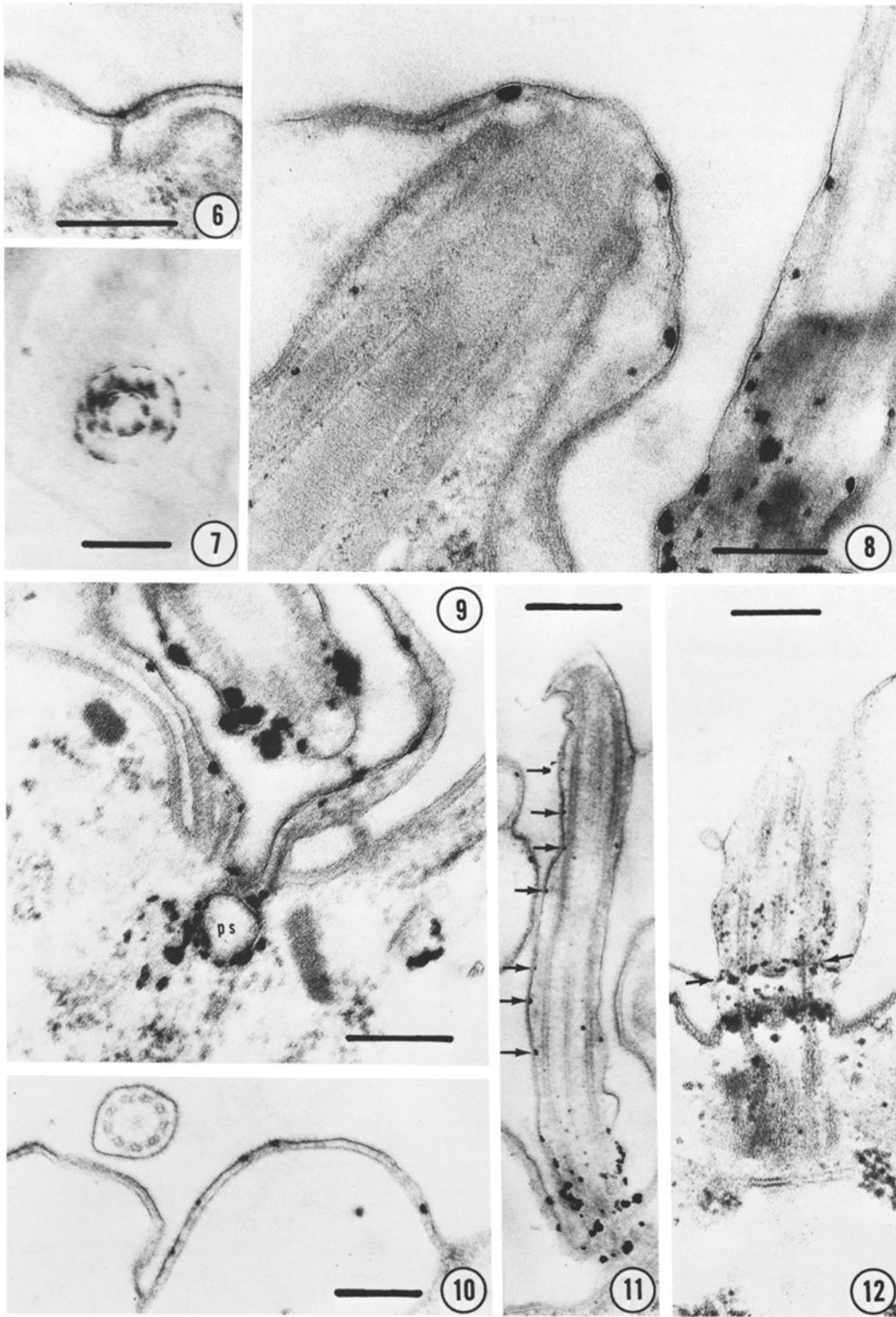
degree of structural or chemical specificity limited to certain cellular sites and not to others.

The distribution pattern of electron-opaque deposits by high Ca^{2+} fixation of *P. Aurelia* was generally similar in the reports of Plattner (37) and the present authors (12). The present study, however, indicates some differences in localization and cation specificity. In addition to showing sites observed to have high frequency of deposits by Plattner (37), this study showed that many deposits also occurred at the terminal plate of the basal body. The uppermost transverse plate of the

FIGURE 13   Cross section through transition zone of cilium of *P. aurelia* 299s fixed in 5 mM Ca^{2+}. Deposits occur opposite nine outer microtubular doublets. Linkers can be seen between microtubular doublets and deposit aggregates. Opposite several outer microtubular doublets, smaller deposits instead of one large one are seen (arrows). Section stained with uranyl acetate. $\times$ 125,000. Bar represents 0.1 μm.

FIGURE 14   Longitudinal section of basal region of cilium of *P. aurelia* 299s fixed in 5 mM Mn^{2+}. Terminal plate of basal body shows large deposits. Section stained with uranyl acetate. $\times$ 27,600. Bar represents 0.5 μm.

FIGURE 15   Cross section at terminal plate of basal body of cilium of *P. aurelia* 299s fixed in 5 mM Mn^{2+}. Deposits associated with the alveolar membranes are in register with microtubular doublets. Deposits also occur on the luminal side of the circle of microtubules, forming an inner ring of deposits (Fig. 17 also illustrates the two rings of divalent cation deposits, one outside and one inside the circle of microtubules). Area between microtubular doublets (arrow) has deposits. Parasomal sac (*ps*) associated with this cilium has deposits. Section stained with uranyl acetate. $\times$ 68,000. Bar represents 0.25 μm.

FIGURE 16   Longitudinal section of cilium of *P. aurelia* 299s fixed in 5 mM Ba^{2+}. Large deposits occur at terminal plate of basal body. Smaller deposits are seen on the cilium above. Section stained with uranyl acetate. $\times$ 45,000. Bar represents 0.25 μm.

FIGURE 17   Cross section of terminal plate of basal body. Unstained preparation of *P. aurelia* 299s fixed in 5 mM Ba^{2+}. $\times$ 35,200. Bar represents 0.5 μm.

FIGURE 18   Longitudinal section of basal region of cilium of *P. aurelia* 299s fixed in 5 mM Sr^{2+}. Terminal plate of basal body has large deposits. Transition zone of cilium also contains deposits on membrane and axoneme. $\times$ 41,600. Bar represents 0.5 μm.

FIGURE 19   Cross section of two cilia immediately above terminal plate of basal body of *P. aurelia* 299s fixed in 5 mM Ca^{2+}. Large deposits on membranes in these profiles are seen between the materials linking membranes to microtubules. Section stained with uranyl acetate and lead citrate. $\times$ 54,400. Bar represents 0.25 μm.

FIGURE 20   Cross section of cilium of *P. aurelia* 299s fixed in 5 mM Mg^{2+}. Deposits are few in number but generally larger than deposits caused by other divalent cations used in this study. Section stained with uranyl acetate and lead citrate. $\times$ 13,200. Bar represents 0.5 μm.

FIGURE 21   Longitudinal section of cilium of *P. aurelia* 299s fixed in 5 mM Ni^{2+}. Specimen postfixed in OsO_4. Section stained with uranyl acetate and lead citrate. $\times$ 32,000. Bar represents 0.5 μm.

FIGURE 22   Basal region of cilium of *P. aurelia* 299s fixed in 5 mM Zn^{2+} contains deposits. This profile also shows large deposits on axosome (arrow). Section stained with uranyl acetate and lead citrate. $\times$ 39,400. Bar represents 0.5 μm.

FIGURE 23   Section through two cilia at terminal plate (right) and above terminal plate (left). *P. aurelia* 299s fixed in 5 mM Mn^{2+}. Large deposits appear on terminal plate. At more distal regions of cilium (left), deposits are much smaller. Compare sizes of Mn deposits with those Ca deposits in Figs. 13 and 19 relative to diameters of cilia. Parasomal sac (*ps*) has deposits. Kinetodesmal fiber (*kf*). Section stained with uranyl acetate. $\times$ 10,400. Bar represents 0.5 μm.

FIGURE 24   Cilium of *P. aurelia* d_495, pawn mutant with defective membrane, shows electron-opaque deposits when fixed in 5 mM Ca^{2+}. Fig. 7 shows that 5 mM Ba^{2+} can also form deposits in d_495 cells. Section stained with uranyl acetate and lead citrate. $\times$ 23,400. Bar represents 0.5 μm.
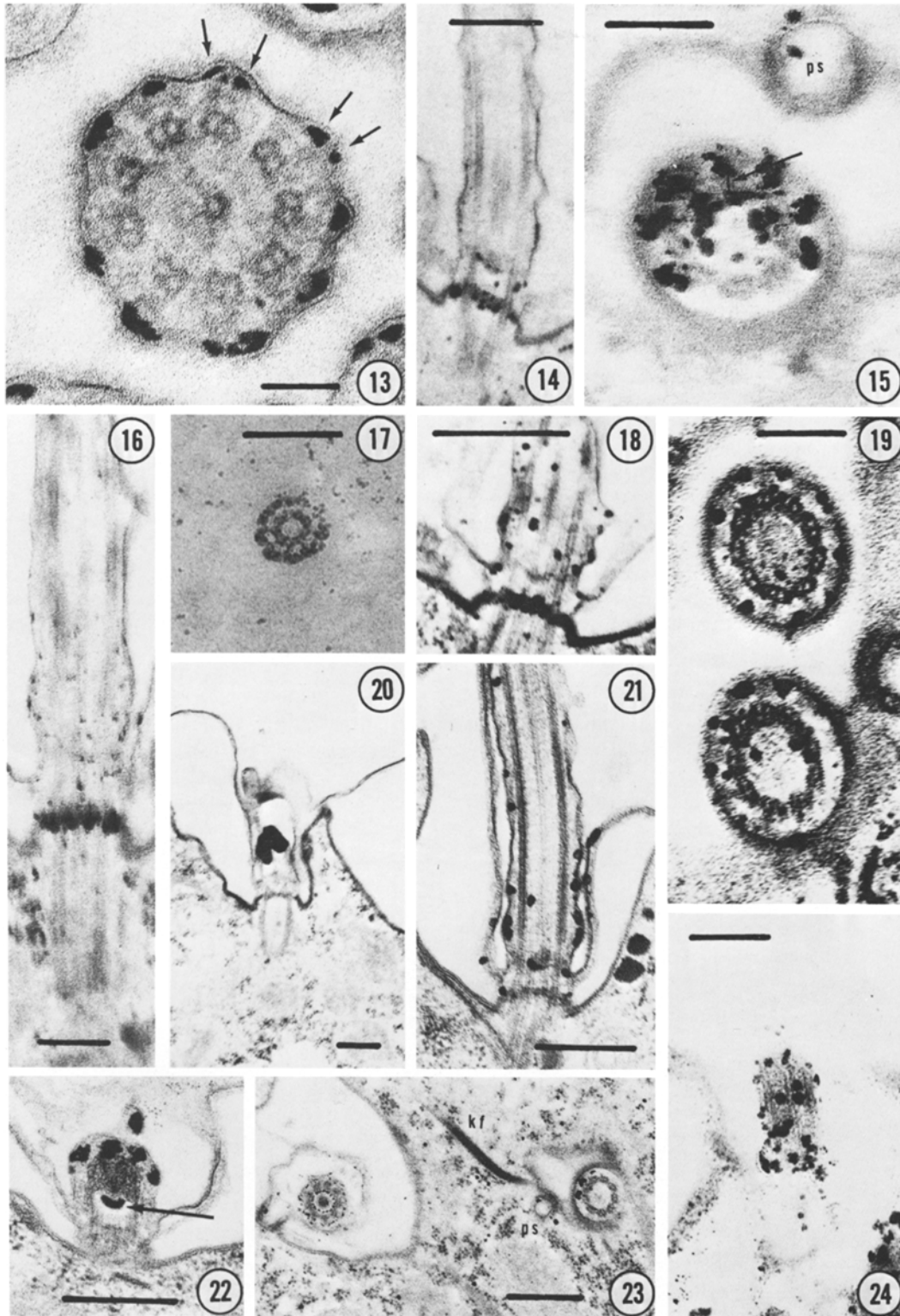
cilium, which is contiguous with the surface membrane and "cups" the axosome (36), also has a divalent cation affinity, but deposits are fewer and smaller than at the terminal plate. The precise structures within the transverse plates and other regions of the transition zone that have apparent divalent cation affinity were not identified in this study. For example, deposits at basal regions of the cilia and deposits on the basal body complex could occur on a variety of linkers or fibrils, but deposits in areas between these linkers or fibrils also occurred.

Electron-opaque deposits seen in a variety of cell types with this technique often coincide with cellular sites exhibiting fibrillar (fuzzy linkers or coats, bridges, bristles, electron-dense material) and/or intramembranous particles as seen by freeze-fracture methods. Intramembranous particles and fibrils have been reported at ciliary sites (37, 43, 48) where deposits occurred (present study). Particles were also found within other membranes of Paramecium at loci that may be correlated with divalent cation deposits reported here. In P. aurelia the trichocyst membrane, surface membrane, and alveolar sac membrane junctions are characterized by intramembranous particles (38, 42) (see Figs. 7 and 8). In Tetrahymena mucocysts there are organelles that are homologous to trichocysts; both extrude their contents upon nonspecific stimulation. The mucocyst-surface fusion site is characterized by a rosette of particles within the surface membrane and an

annulus of particles within the mucocyst membrane (42). The deposition of Ca at regions where trichocyst and surface membranes fuse could be related to the well-documented role of calcium in the control of exocytosis (8). In Paramecium caudatum, filamentous material connects disc-shaped vesicle membranes to microtubules (5). The vesicle membranes contain intramembranous particles (4), and participate in membrane-membrane fusion with the cytopharyngeal surface membrane during endocytosis (see Fig. 4). The parasomal sac membrane of ciliates is covered by a fuzzy material on its cytoplasmic surface (1) (see Fig. 9). Alveolar septa between adjacent alveolar sacs are associated with membrane particles in P. aurelia (38). Divalent cation deposits occurred at all the sites discussed above.

In other cell types studied by this fixation technique, intramembranous particles and/or fibrillar material can be correlated with deposit sites. In invertebrate nerve axons, aggregates of intramembranous particles occur (35) (J. Metuzals, personal communication), and Ca deposits are observed (19, 32, 34). Gap junctions contain intercalated membrane particles (15, 26, 40), and Ca deposits (24). Transverse tubules connect to terminal cisternae by electron-dense "feet" in striated muscle (13), and Ca deposits have been observed on transverse tubular membranes (39). Platelet membranes are associated with fibrils and particles (11, 50) and Ca deposits (44). Synaptic vesicles are associated with filamentous coats (18)

FIGURE 25-30 Emission spectra of microprobe analysis on unstained thick sections of P. aurelia. The two Ti peaks on each are due to K_α and K_β emissions from specimen holder. Silicon detected in each analysis probably from vacuum pump oil of instrument.

FIGURE 25 Microprobe analysis of electron-opaque deposits in cells fixed in 5 mM Ca^{2+} shows increased Ca and Cl. In this set of analyses, more P was shown in deposits (cf. Fig. 26).

FIGURE 26 Microprobe analysis of an area without deposits in cell fixed in 5 mM Ca^{2+}. See Fig. 25.

FIGURE 27 Microprobe analysis of deposits of cell different from that of Fig. 25. In this set (cf. Fig. 28), S was more concentrated in deposits. Phosphorus was only slightly more concentrated. As in Figs. 25 and 26, Ca and Cl are concentrated in deposits.

FIGURE 28 Microprobe analysis of an area without deposits in cell (Fig. 27) fixed in 5 mM Ca^{2+}. Cf. Fig. 27.

FIGURE 29 Electron-opaque deposits in cells fixed in 5 mM Mn^{2+} are enriched in Mn and Cl. Phosphorus enrichment is also detected in this set of analyses. Cf. Fig. 30.

FIGURE 30 Microprobe analysis of cell (Fig. 29) of an area without deposits. Cell fixed in 5 mM Mn^{2+}. Cf. Fig. 29.

and Ca deposits (6, 39). Such correlations between cation affinity and protein or lipoprotein particles within membranes, which may attach to fibrillar material, could have significance in the understanding of several cellular functions including (*a*)

mechanisms involved with membrane "gates" and regulation of permeabilities to certain ions or compounds, (*b*) modification of contractile processes by a variety of anchoring sites which may be differentially affected, (*c*) maintenance of the cell
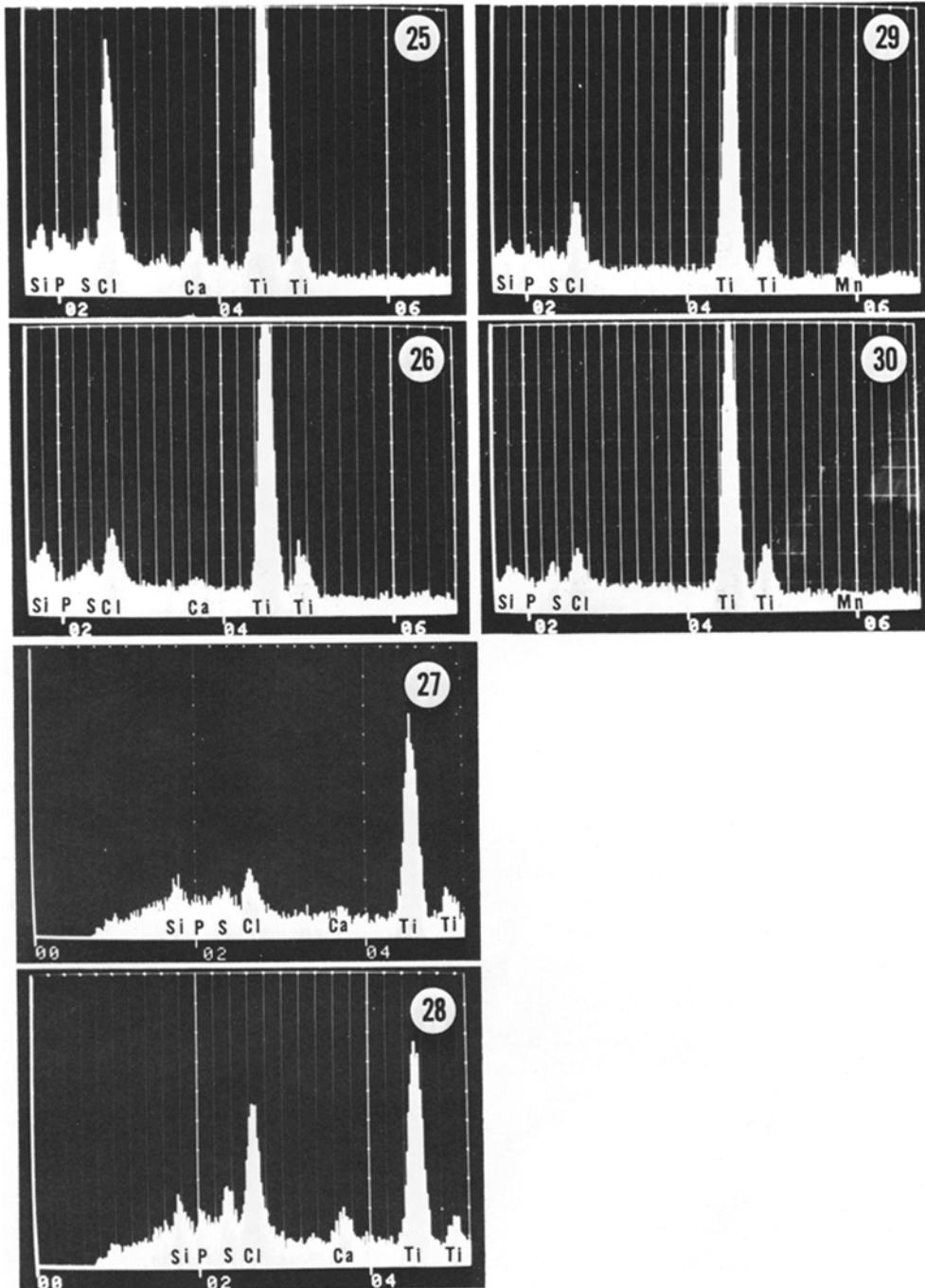
architecture by membrane-membrane connections, or (*d*) membrane growth by insertion of components at specific sites.

These sites have been shown to have divalent cation affinity, but the specificity is not restricted to Ca^{2+}. They appear to be specific for divalent cations since mono- and trivalent cations do not cause electron-dense deposits (12, 33, 34, 37, and present study). All divalent cations tested in this study (Ca^{2+}, Mg^{2+}, Mn^{2+}, Sr^{2+}, Ba^{2+}, Zn^{2+}, and Ni^{2+}) caused deposits. This study confirmed the finding of Oschman et al., who worked with insect gut epithelial cells (33) and squid axons (34), that a variety of divalent cations, including Mg^{2+}, can substitute in this procedure to give deposits. Politoff et al. (39) also found that Co^{2+} was able to substitute for Ca^{2+} in forming deposits at the synaptic vesicle membrane. In contrast, Plattner (37) did not find Mg^{2+} deposition in *P. aurelia* and concluded that binding sites were strictly specific for Ca^{2+}.

The heavier deposition by Sr^{2+}, Ba^{2+}, and Mn^{2+} seen on the terminal plate may be related to the observation that in *Paramecium*, Sr^{2+} and Ba^{2+} can substitute for Ca^{2+} in causing ciliary reversal and carrying the active inward current associated with the stroke reorientation. *Paramecium* responds more strongly to these cations than to Ca^{2+}, and the cell membrane exhibits an action potential with Sr^{2+} and Ba^{2+} whereas Ca^{2+} yields only a graded response (28). Many large deposits at the terminal plate may also be related to the observation that Ba^{2+}, Sr^{2+} and Mn^{2+} were able to substitute for Ca^{2+} (C. Roberts and E. S. Kaneshiro, unpublished observations) in the method for mass deciliation of *Tetrahymena* pretreated with glycerol and EDTA (21).

The deposits contain the cation added to the fixative. Microprobe analyses confirmed the presence of Mn in deposits in high Mn^{2+}-fixed cells and of Ca in high Ca^{2+}-fixed cells. Chlorine was also present in greater amounts in Ca and Mn deposits when compared to background, which suggests that deposit formation involves the salts of divalent cations. Chlorine is present in the embedding medium (44), which could account for the detection of this element in areas without deposits. Of the reports on deposits caused by high Ca^{2+} fixation and analyzed by microprobe techniques, all showed enrichment of Ca and P (14, 19, 32, 44). In the present study, P enrichment was not consistently detected and thus argues against the idea that deposits are formed from Ca^{2+} interact-

ing with the phosphate released at ATPase sites (32). The present study does not eliminate P precipitation as a mechanism for deposit formation but supports the notion that deposits represent cationic binding sites and are formed from interactions with organic substructures (19, 37). The S enrichment detected in some microprobe analyses may represent aggregation of S-rich proteins at deposit sites. The role of S at Ca-binding sites in *Paramecium* is consistent with the presence of S and the importance of —SH functions in several catalytic, binding, or transport sites, e.g., ATPase activity of muscle heavy meromyosin and actin-myosin interaction, or Ca uptake activity of sarcoplasmic reticulum. The large number of divalent cations accumulated at each site which permits electron microscope visualization and microprobe analysis suggests that mechanisms other than those involving a stoichiometric relationship with an individual protein molecule are involved (32). A significant conclusion from all studies on high Ca^{2+} fixation is that divalent cations bind at specific morphological sites. The initial binding of divalent cations at specific membrane sites could then cause structural changes and increased membrane permeability at these restricted loci. After permeability changes at these sites, the influx of divalent cation or its salt, which could explain the enrichment of Cl in all microprobe analyses of deposits in this study, could flood these areas until they become electron opaque. Glutaraldehyde could preserve the subcellular compartmentalization of the divalent cation- or salt-rich sites and, thus, the maintenance of discrete deposits. This dense accumulation of divalent cations could conceivably occur in the living organism since the concentration of Ca^{2+} in the fixative is well within the physiological range (0.1–10 mM) for *Paramecium* (9). Also, Plattner (37) reported that cells exposed to 5 mM Ca^{2+} for 10 min, then fixed with glutaraldehyde, exhibited deposits. Alternatively, glutaraldehyde, by its capacity as a cross-linker, could cause aggregation of binding sites and bound divalent cations into electron-opaque deposits. Aldehyde fixation, however, alters divalent cation-accumulating mechanisms since deposits were not present if cells were treated with 5 mM Ca^{2+} after fixation in Ca^{2+}-free fixative (37) (present study). Also, this study has shown that only physiologically active cells contain deposits since only ciliates which were actively swimming at the time of fixation showed deposits. This indicates that deposit mechanisms are also altered by ad-

verse physiological conditions. It is possible that cationic binding sites in moribund or immotile ciliates have a decreased affinity for Ca^{2+} and/or a decreased availability of ATP. If the absence of deposits in these cells were specifically correlated with ATP depletion, this, among other possibilities discussed above, could implicate ATP in altering the relative Ca-binding capacities of the sites.

The inability of this study to resolve differences between cells exhibiting different locomotory behavior (and therefore different orientations of ciliary effective strokes) as well as differences between membrane-gating mutants (22) vs. normal ciliates indicates that the biochemical or physiological differences involved in ciliary reversal may be more subtle than the resolution offered by these methods. It is possible that structural or biochemical loci of divalent cation action were identified by this study but that the sites are only slightly modified in different states. It is also possible that gating sites involved in eventual ciliary reversal have been identified but that they misfunction in pawn mutants by yet unidentified accessory factors.

REFERENCES

1. ALLEN, R. D. 1967. Fine structure, reconstruction and possible functions of components of the cortex of *Tetrahymena pyriformis. J. Protozool.* **14**:553-565.
2. ALLEN, R. D. 1969. The morphogenesis of basal bodies and accessory structures of the cortex of the ciliated protozoan *Tetrahymena pyriformis. J. Cell Biol.* **40**:716-733.
3. ALLEN, R. D. 1971. Fine structure of membranous and microfibrillar systems in the cortex of *Paramecium caudatum. J. Cell Biol.* **49**:1-20.
4. ALLEN, R. D. 1974. Food vacuole membrane growth with microtubule-associated membrane transport in *Paramecium. J. Cell Biol.* **63**:904-922.
5. ALLEN, R. D. 1975. Evidence for firm linkages between microtubules and membrane-bounded vesicles. *J. Cell Biol.* **64**:497-503.
6. BOYNE, A. F., T. P. BOHAN, and T. H. WILLIAMS. 1974. Effects of calcium-containing fixation solu-

7. CONNER, R. L., S. G. CLINE, M. J. KOROLY, and B. HAMILTON. 1966. A method of harvesting mass cultures of *Tetrahymena pyriformis. J. Protozool.* **13**:377-379.
8. DOUGLAS, W. W. 1974. Involvement of calcium in exocytosis and the exocytosis-vesiculation sequence. *Biochem. Soc. Symp.* **39**:1-28.
9. ECKERT, R. 1972. Bioelectric control of ciliary activity. *Science (Wash. D. C.).* **176**:473-481.
10. ECKERT, R., and H. MACHEMER. 1975. Regulation of ciliary beat frequency by the surface membrane. *In* Molecules and Cell Movement. S. Inoué and R. E. Stephens, editors. Raven Press, New York. 151-163.
11. FEAGLER, J. R., T. W. TILLACK, D. D. CHAPLIN, and P. W. MAJERUS. 1974. The effects of thrombin on phytohemagglutinin receptor sites in human platelets. *J. Cell Biol.* **60**:541-553.
12. FISHER, G. W., and E. S. KANESHIRO. 1975. Ultrastructural localization of calcium deposits in cilia of *Paramecium aurelia. J. Cell Biol.* **67**(2, Pt. 2):115 *a* (Abstr.).
13. FRANZINI-ARMSTRONG, C. 1974. Freeze fracture of skeletal muscle from the tarantula spider. Structural differentiation of sarcoplasmic reticulum and transverse tubular system membrane. *J. Cell Biol.* **61**:501-513.
14. GAMBETTI, P., S. E. ERULKAR, A. P. SOMLYO, and N. K. GONATAS. 1975. Calcium-containing structures in vertebrate glial cells. *J. Cell Biol.* **64**:322-330.
15. GILULA, N. B., O. R. REEVES, and A. STEINBACH. 1972. Metabolic coupling, ionic coupling and cell contacts. *Nature (Lond.).* **235**:260-265.
16. GOLDSTEIN, S. F. 1974. Isolated, reactivated and laser-irradiated cilia and flagella. *In* Cilia and Flagella. M. A. Sleigh, editor. Academic Press, Inc., New York. 111-130.
17. GREBECKI, A. 1965. Role of Ca^{2+} ions in the excitability of protozoan cell. Decalcification, recalcification, and the ciliary reversal in *Paramecium caudatum. Acta Protozool.* **3**:275-289.
18. HEUSER, J. E., and T. S. REESE. 1973. Evidence for recycling of synaptic vesicles membranes during transmitter release at the frog neuromuscular junction. *J. Cell Biol.* **57**:315-344.
19. HILLMAN, D. E., and R. LLINÁS. 1974. Calcium-containing electron-dense structures in the axons of the squid giant synapse. *J. Cell Biol.* **61**:146-155.
20. HUFNAGEL, L. A. 1969. Cortical ultrastructure of *Paramecium aurelia.* Studies on isolated pellicles. *J. Cell Biol.* **40**:779-801.
21. KANESHIRO, E. S., E. RAY, and R. L. CONNER. 1971. Lipids of cilia and ciliary membranes of *Tetrahymena pyriformis:* effects of ergosterol. *J. Protozool.* **18**(Suppl.):9. (Abstr.).

tions on cholinergic synaptic vesicles. *J. Cell Biol.* **63**:780-795.

22. Kung, C., and R. Eckert. 1972. Genetic modification of electrical properties in an excitable membrane. *Proc. Natl. Acad. Sci. U. S. A.* **69**:93-97.

23. Kung, C., and Y. Naitoh. 1973. Calcium-induced ciliary reversal in the extracted models of "pawn", a behavioral mutant of *Paramecium. Science* (*Wash. D. C.*). **179**:195-196.

24. Larsen, W. J. 1974. Calcium deposition on cytoplasmic faces of gap junctions. *J. Cell Biol.* **63**(2, Pt. 2):1862 *a.* (Abstr.).

25. Luft, J. H. 1961. Improvements in epoxy resin embedding methods. *J. Biophys. Biochem. Cytol.* **9**:409-411.

26. McNutt, N. S., and R. S. Weinstein. 1970. The ultrastructure of the nexus, a correlated thin-section and freeze-cleave study. *J. Cell Biol.* **47**:666-688.

27. Naitoh, Y. 1973. Role of bound calcium in the control of cilia. *In* Behavior of Micro-organisms. A. Perez-Miravete, editor. Plenum Press, New York. 127-144.

28. Naitoh, Y., and R. Eckert. 1968. Electrical properties of *Paramecium caudatum:* all-or-none electrogenesis. *Z. Vgl. Physiol.* **61**:453-472.

29. Naitoh, Y., and R. Eckert. 1974. The control of ciliary activity in protozoa. *In* Cilia and Flagella. M. A. Sleigh, editor. Academic Press, Inc., New York. 305-352.

30. Naitoh, Y., and H. Kaneko. 1972. Reactivated Triton-extracted models of *Paramecium:* modification of ciliary movement by calcium ions. *Science* (*Wash. D. C.*). **176**:523-524.

31. Noirot-Tomothée, C. 1968. The parasomal sacs are sites of pinocytosis. Experimental study done with thorotrast in *Trichodinopsis paradoxa. C. R. Hebd. Sebd. Acad. Sci. Ser. D. Sci. Nat.* **267**:2334-2336.

32. Oschman, J. L., T. A. Hall, P. D. Peters, and B. J. Wall. 1974. Association of calcium with membranes of squid giant axon. Ultrastructure and microprobe analysis. *J. Cell Biol.* **61**:156-165.

33. Oschman, J. L., and B. J. Wall. 1972. Calcium binding to intestinal membranes. *J. Cell Biol.* **55**:58-73.

34. Oschman, J. L., and B. J. Wall. 1974. Association of divalent cations with membranes of squid giant axon. *Biol. Bull.* (*Woods Hole*). **147**:493 *a.* (Abstr.).

35. Peracchia, C. 1974. Excitable membrane ultrastructure. 1. Freeze-fracture of crayfish axons. *J. Cell Biol.* **61**:107-122.

36. Pitelka, D. R. 1974. Basal bodies and root structures. *In* Cilia and Flagella. M. A. Sleigh, editor. Academic Press, Inc., New York. 437-470.

37. Plattner, H. 1975. Ciliary granule plaques: membrane-intercalated particle aggregates associated with Ca^{2+}-binding sites in *Paramecium. J. Cell Sci.* **18**:257-269.

38. Plattner, H., T. Miller, and L. Bachmann. 1973. Membrane specialization in the form of regular membrane-to-membrane attachment sites in *Paramecium.* A correlated freeze-etching and ultrathin-sectioning analysis. *J. Cell Sci.* **13**:687-719.

39. Politoff, A. L., S. Rose, and G. D. Pappas. 1974. The calcium binding sites of synaptic vesicles of the frog sartorius neuromuscular junction. *J. Cell Biol.* **61**:818-823.

40. Revel, J. P., A. G. Yee, and A. J. Hudspeth. 1971. Gap junctions between electrotonically coupled cells in tissue culture and in brown fat. *Proc. Natl. Acad. Sci. U. S. A.* **68**:2924-2927.

41. Reynolds, E. S. 1963. The use of lead citrate at high pH as an electron-opaque stain in electron microscopy. *J. Cell Biol.* **17**:208-212.

42. Satir, B., C. Schooley, and P. Satir. 1973. Membrane fusion in a model system. Mucocyst secretion in *Tetrahymena. J. Cell Biol.* **56**:153-176.

43. Sattler, C. A., and L. A. Staehelin. 1974. Ciliary membrane differentiations in *Tetrahymena pyriformis. Tetrahymena* has four types of cilia. *J. Cell Biol.* **62**:473-490.

44. Skaer, R. J., P. D. Peters, and J. P. Emmines. 1974. The localization of calcium and phosphorus in human platelets. *J. Cell Sci.* **15**:679-692.

45. Soldo, A. T., G. A. Godoy, and W. J. van Wagtendonk. 1966. Growth of particle-bearing and particle-free *Paramecium aurelia* in axenic culture. *J. Protozool.* **13**:492-497.

46. Sonneborn, T. M. 1970. Methods in *Paramecium* research. *In* Methods in Cell Physiology. D. Prescott, editor. Academic Press, Inc., New York. Vol. 14.

47. Spurr, A. R. 1969. A low viscosity epoxy resin embedding medium for electron microscopy. *J. Ultrastruct. Res.* **26**:31-43.

48. Warner, F. D. 1974. The fine structure of the ciliary and flagellar axoneme. *In* Cilia and Flagella. M. A. Sleigh, editor. Academic Press, Inc., New York. 11-38.

49. Watson, M. R., and J. M. Hopkins. 1962. Isolated cilia from *Tetrahymena pyriformis. Exp. Cell Res.* **28**:280-295.

50. Zucker-Franklin, D. 1970. The submembranous fibrils of human blood platelets. *J. Cell Biol.* **47**:293-299.